HHS Public Access

Author manuscript

Nat Neurosci. Author manuscript; available in PMC 2012 November 01.

Published in final edited form as:

Nat Neurosci. ; 15(5): 700–702. doi:10.1038/nn.3079.

Tanycytes of the Hypothalamic Median Eminence Form a Diet-Responsive Neurogenic Niche

Daniel A. Lee[1,7], **Joseph L. Bedont**[1,†], **Thomas Pak**[1,†], **Hong Wang**[1], **Juan Song**[3,7], **Ana Miranda-Angulo**[1,8], **Vani Takiar**[1], **Vanessa Charubhumi**[1], **Francesca Balordi**[9], **Hirohide Takebayashi**[10], **Susan Aja**[1,5], **Eric Ford**[4], **Gordon Fishell**[9], and **Seth Blackshaw**[1,2,3,6,7]

[1]Solomon H. Snyder Department of Neuroscience, Johns Hopkins University School of Medicine, Baltimore, MD, USA 21287

[2]Department of Ophthalmology, Johns Hopkins University School of Medicine, Baltimore, MD, USA 21287

[3]Department of Neurology, Johns Hopkins University School of Medicine, Baltimore, MD, USA 21287

[4]Department of Radiation Oncology, Johns Hopkins University School of Medicine, Baltimore, MD, USA 21287

[5]Center for Metabolism and Obesity Research, Johns Hopkins University School of Medicine, Baltimore, MD, USA 21287

[6]Center for High-Throughput Biology, Johns Hopkins University School of Medicine, Baltimore, MD, USA 21287

[7]Institute for Cell Engineering, Johns Hopkins University School of Medicine, Baltimore, MD, USA 21287

[8]Universidad de Antioquia, Medellin, Colombia

[9]Neuroscience Program and the Department of Cell Biology, Smilow Research Center, New York University School of Medicine, New York, NY 10016, USA

[10]Division of Neurobiology and Anatomy, Graduate School of Medical and Dental Sciences, Niigata University, Niigata 951-8510, Japan

Abstract

Adult hypothalamic neurogenesis has been recently reported, but the cell of origin and function of these newborn neurons are unknown. We utilize genetic fate mapping to show that median

Correspondence to: Seth Blackshaw.

†These authors contributed equally.

Author contributions:

D.A.L and S.B. designed experiments. D.A.L., J.L.B., T.P., V.T., J.S., H.W., A.M.A., E.F., V.C., and S.A. performed experiments. D.A.L., J.L.B., T.P., A.M.A., V.C., S.A., and S.B. analyzed data. F.B., H.T., and G.F. contributed transgenic mice. D.A.L. and S.B. wrote the manuscript.

eminence tanycytes generate newborn neurons; blocking this neurogenesis alters weight and metabolic activity in adult mice. These findings describe a previously unreported neurogenic niche within the mammalian hypothalamus with important implications for metabolism.

Several recent studies have reported neurogenesis in postnatal and adult mammalian hypothalamus[13]. The cell of origin and function of these newborn neurons, however, are unknown. Hypothalamic radial glia-like ependymal cells, named tanycytes, are a strong progenitor cell candidate that resides within the ventral hypothalamic ventricular zone[4]. Tanycytes are known to express neural stem cell markers such as Nestin[5]; we have shown that tanycytes also express Notch pathway components and hypothalamic progenitor-specific transcription factors[6] like Rax (SFig. 1). Nonetheless, tanycytes have not been previously shown to proliferate substantially or give rise to other cell-types *in vivo*.

We quantified cell proliferation in mouse hypothalamus, conducting bromodeoxyuridine (BrdU) labeling in postnatal and adult mice. We observed substantial enrichment of $BrdU^+$ ependymal layer cells at the base of the third ventricle (3V) of the median eminence (MEm) relative to other hypothalamic regions (Fig. 1a–b, SFig. 2). We named this proliferative domain the hypothalamic proliferative zone (HPZ) and determined by position, morphology, and co-expression of tanycyte markers[5] Nestin, Sox2, and Vimentin that proliferating cells within this domain were β2-tanycytes (Fig. 1c, SFig. 2b–d).

Concurrently, MEm neuronal numbers increased markedly from PD7 65, suggesting HPZ cell proliferation reflects an active neurogenic zone (SFig. 3a). To address this, we immunostained for BrdU and the pan-neuronal marker Hu, observing that 4.5%±1.1 of MEm Hu^+ neurons co-labeled with BrdU, compared to a much smaller fraction of Hu^+BrdU^+ neurons in other hypothalamic regions (Fig. 2b, SFig. 3b). Furthermore, BrdU co-expressed with other markers of mature hypothalamic neurons (SFig. 3c–g). Fasting activates c-fos expression in ventrobasal hypothalamic neurons[7], and we observed $Hu^+BrdU^+c\text{-}fos^+$ MEm neurons (SFig. 4a,b,f). Similarly, leptin injection activates STAT3 in hypothalamic neurons[8], and 21.2%±4.2 (72/366 total counts for n=4) of newborn Hu^+BrdU^+ neurons expressed pSTAT3 in leptin-injected BrdU-treated mice, compared to 3.4%±1.7 (8/244 total counts for n=3) for fasted control mice (SFig. 4c–e). These data suggest newborn MEm neurons are functionally active.

Numerous studies have shown that high-fat diet (HFD) during adolescent periods can lead to long-term food intake and weight changes[9]. To determine whether these changes correlated with hypothalamic neurogenesis, we conducted daily BrdU labeling from PD6 14, PD15 23, or PD45 53 in mice fed normal chow or HFD, examining mice one month after the initial BrdU injection (P35, 45, or 75, respectively) (Fig. 2c). We observed no significant difference in neurogenesis between normal chow or HFD-fed PD35 mice; however, neurogenesis rates quadrupled in adult (PD75) HFD-fed mice compared to controls, with BrdU co-labeling reaching 5.9%±1.6 of Hu^+ MEm neurons (114/1941 total neurons for n=4) (Fig. 2c, STable 1). Thus, prolonged dietary changes can profoundly affect HPZ neurogenesis into adulthood.

To address whether β2-tanycytes directly give rise to neurons *in vivo*, we bred transgenic Nestin:CreER^{T2} driver[10] and ROSA26stopYFP reporter[11] to inducibly and selectively fate-map tanycytes and their progeny (Fig. 2d–f). Nestin:CreER^{R26stopYFP} mice did not express yellow fluorescent protein (YFP) in ventral hypothalamus without 4-hydroxytamoxifen (4-OHT) (SFig. 5a–b). Immediately following PD4 4-OHT induction, Nestin:CreER^{R26stopYFP} permanently labeled Nestin^{+} tanycytes with YFP (Fig. 2e); 17.9%±1.7 (1457/7949 total cells for n=3) of Sox2^{+} β2-tanycytes were labeled (SFig. 5c–e). Importantly, we observed no co-labeling of YFP and the astrocyte marker glial fibrillary acidic protein or Hu immediately after induction (SFig. 5f–g). At PD35, one month post-induction, a substantial fraction of Hu^{+} MEm neurons were labeled with YFP (7.8%±0.6; 160/2097 total neurons for n=4; Fig. 2f, SFig. 5i), suggesting that β2-tanycytes give rise directly to neurons *in vivo*. When PD35 Nestin:CreER^{R26stopYFP} mice were fasted, Hu^{+}YFP^{+}c-fos^{+} MEm neurons were detected (SFig. 5h), suggesting that newborn neurons are functionally active. We also observed a much smaller fraction of Hu^{+}YFP^{+} neurons in hypothalamic regions outside MEm, with the MEm showing a 43-fold higher level of neurogenesis compared to the arcuate nucleus following correction for the percentage of tanycytes labeled by the Nestin:CreER^{T2} driver (STable 2). Parallel negative control experiments which prospectively labeled Olig2^{+} oligodendrocyte precursor cells (OPCs)[12], suggested that OPCs were not an appreciable source of newborn neurons (SFig. 6). Taken together, this data suggests that β2-tanycytes are highly neurogenic.

We next probed the functional role of adult born MEm neurons, using focal CT-guided irradiation[13] to selectively inhibit adult MEm neurogenesis while sparing other neurogenic regions (Fig 3a–c, SFig. 7a–c). Targeting of ventrobasal hypothalamus was guided by iodine contrast CT scans, and confirmed by X-ray dosimetry film (Fig. 3b, SFig. 7b). Immunostaining for γH2AX a sensitive readout of double-stranded DNA breaks that correlates strongly with radiation dosage[14], indicated that ventrobasal hypothalamus was targeted while other neurogenic niches were spared (Fig. 3c). Irradiated HFD-fed adult mice exhibited ~85% inhibition of MEm neurogenesis compared with sham-treated controls (Fig. 3e). Surprisingly, HFD-fed adults gained significantly less weight and fat mass when irradiated compared with sham controls (SFig. 7d–e). Furthermore, oxygen consumption, energy expenditure, and total activity were significantly elevated by irradiation of ventrobasal hypothalamus (Fig. 3f–g, SFig. 7f–g). Taken together, these data suggest that adult MEm neurogenesis plays a functional role in weight regulation.

In this study, we observed that levels of neurogenesis in MEm were more than 5-fold higher than other hypothalamic regions, and that newborn neurons are derived from β2-tanycytes. The potential physiological importance of this tanycyte neural progenitor pool is magnified by its position outside the blood-brain barrier and innervation by neurosecretory cells. Changes in the number and connectivity of MEm neurons may thus have an impact disproportionate to their number. While we observe low levels of neurogenesis in other hypothalamic regions, lineage analysis shows that very few of these cells are derived from Nestin^{+} tanycytes. These data also suggest that other as yet unidentified non-tanycyte progenitor cell populations may exist in postnatal hypothalamus.

Postnatal MEm neurogenesis is substantially enhanced by HFD, and may lead to long-term changes in feeding and metabolism. HFD activation of MEm neurogenesis continues into adulthood raising the possibility that this process might modulate hypothalamic neural circuitry late in life. Previous studies have shown that whole brain X-irradiation leads to long-lasting changes in body weight[15]. We find that selectively inhibiting adult neurogenesis in the ventrobasal hypothalamus of HFD-animals leads to attenuated weight gain and higher levels of activity relative to controls. This suggests that MEm neurogenesis induced by overfeeding reduces baseline energy consumption and promotes energy storage in the form of fat. Such a response is likely adaptive in wild animals for which rich food sources are rare, but maladaptive in laboratory housed mice. These findings raise the question of whether other dietary cues can regulate MEm neurogenesis, and whether this effect is observed in humans.

Online Material and Methods

Animals

5 week old or pregnant female C57BL/6 mice were obtained from Charles River and housed in a 14/10-h light-dark cycle with free access to chow (Teklad F6 Rodent Diet 8664, Harlan Teklad, Madison, WI) and water. Where indicated, animals were provided with a high-fat diet (HFD) (60% of the calories as fat, Rodent Diet – Catalog #: D12492i, Research Diets, New Brunswick, NJ) *ad libitum* from PD5 35. Prior to weaning, this diet was supplied to nursing mothers. Normal chow and HFD diet administration for age and diet-dependent effect experiment visualized in Figure 2c. All mice used in these studies were maintained and euthanized according to protocols approved by the Institutional Animal Care and Use Committee at the Johns Hopkins School of Medicine.

Inducible Cre Lines and Mice Breeding—Nestin:CreER^{T2} mice were a generous gift of G. Fishell (New York University, New York, NY) and genotyped as previously described[10]. These mice were backcrossed at least six generations into C57BL/6 strain, and then crossed to the ROSA26stopYFP reporter line obtained from the Jackson Laboratory (Bar Harbor, ME). Double heterozygous PD 4.5 pups (3 3.4 grams body weight) received 0.2mg 4-hydroxytamoxifen (4-OHT). Olig2:CreER mice were a generous gift of H. Takebayashi (Niigata University, Kumamoto, Japan), and crossed to the ROSA26stopYFP line. Double heterozygous PD4.5 pups received 0.25mg 4-OHT. Sham oil vehicle control was performed on both sets of mutant animals in parallel with 4-OHT induction experiments.

POMC:Cre mice[8] obtained from Jackson Laboratory (Bar Harbor, ME), were crossed to the Z/EG (C57BL/6 background) reporter line (Jackson Laboratory; Bar Harbor, ME). Double heterozygous postnatal day pups received BrdU pulses on PD10 to PD18 as indicated below.

Reagents

Bromodeoxyuridine (BrdU) and 4-hydroxytamoxifen (4-OHT)—Where indicated, animals received bromodeoxyuridine (BrdU; Sigma) administrated in the morning and evening by intraperitoneal injection at 50 mg/kg of body weight from P10 to PD18. For

examination of temporal changes in median eminence (MEm) neurogenesis (Fig. 2c), mice were administered BrdU by i.p. injection for 9 days for the dates indicated. For BrdU saturation studies examining proliferative changes in the HPZ over time (Supplementary Fig. 2f), 50 mg/kg of BrdU was administered by i.p. injection every 2 hrs for 12 hrs. Mice were subsequently sacrificed at the end of this 12-hour period. 4-hydroxytamoxifen (4-OHT)(Sigma, St. Louis, MO) was prepared as a 50mg/ml stock solution in anhydrous ethanol. 4-OHT was sonicated in a heated water bath, and 100ul of dissolved solution was pipetted into 500ul of corn oil (Sigma, St. Louis, MO), and vortexed. Ethanol was evaporated off by heated vacuum centrifuge. 4-OHT/oil solution was administered to mice by oral gavage.

Tissue processing and antibodies—Postnatal and adult mice were sacrificed, perfused with 2% or 4% PFA/PBS, and cryoprotected as previously described[10]. Serial sections (40 μm thick) were collected and stored at −20° C. Free-floating sections were immunostained using the following primary antibodies and working concentrations: sheep polyclonal anti-BrdU (1:500, Abcam, Cambridge, MA), rat monoclonal anti-BrdU (1:200, Accurate, Westbury, NY), rabbit polyclonal anti-Sox2 (1:1500 Chemicon, Temecula, CA), mouse monoclonal anti-Nestin (1:100, BD Pharmingen), mouse monoclonal anti-Vimentin (1:100, DSHB), mouse monoclonal anti-Hu (5μg/ml, Molecular Probes, Carlsbad, CA), mouse monoclonal anti-GFAP (1:500, Chemicon, Temecula, CA), rabbit polyclonal anti-GFAP (1:500, DAKO), rabbit polyclonal anti-Olig2 (1:500, Chemicon, Temecula, CA), rabbit polyclonal anti-NG2 (1:500, generous gift from Bill Stallcup), goat polyclonal anti-Dcx (1:200, Santa Cruz, Santa Cruz, CA), rabbit polyclonal anti-pSTAT3 (1:2000, Cell Signaling, Beverly, MA), rabbit polyclonal anti-GFP (1:1000, Invitrogen), chicken polyclonal anti-GFP (1:500, AvesLab, Oregon), mouse monoclonal anti-GAD6 (1:200, DSHB), rabbit polyclonal anti-MAP2 (1:50, Sigma), rabbit polyclonal anti-c-fos (1:500, Santa Cruz). Double and triple staining was visualized with Alexa Fluor 488-, Alexa Fluor 555-, Alexa Fluor 568-, Alexa Fluor 594-, Alexa Fluor 633-conjugated secondary antibodies (1: 500, Molecular Probe, Carlsbad, CA). 4′,6-diamidino-2-phenylindole (DAPI) was used as a nuclear counterstain, unless otherwise noted.

Immunohistochemistry and *in situ* hybridization

For BrdU immunostaining, sections were first incubated in 2N HCl at 37°C for 30 min, and rinsed in 0.1 M boric acid (pH 8.5) at room temperature for 10 min. Sections were then rinsed in PBST, blocked for 5 min in SuperBlock (ScyTek), and incubated overnight with in anti-BrdU antibody in 5% normal horse serum in PBS/0.16% Triton X-100 at 4°C in blocking solution. Sections were washed in PBST, incubated with secondary antibodies in blocking solution at RT for 2 h, washed in PBST, mounted on Superfrost Plus slides (Fisher, Hampton, NH), and coverslipped with Gelvatol mounting medium. *In situ* hybridization techniques and sequences of probes (i.e. NPY) used, have been previously described[6].

Cell quantification—All tissue sections used for quantification were imaged using confocal microscopy (Meta 510, Zeiss Microscopy). MEm cells were counted. The dorsal-ventral boundary of the cells counted was the third ventricle (3rdV) floor and the ventral edge of the external layer of the MEm. The lateral boundaries were a 20um medial inset off

the corner of the 3rdV. In only one instance (Supplementary Fig. 4, $Hu^+/pSTAT3^+/BrdU^+$ counts), the lateral boundaries were set at the corners of the median eminence. MEm dorsal and ventral boundaries remained identical to as previously described. For examination of the number of proliferative cells within the ependymal layer, $BrdU^+$ cells in the ependymal layer of the 3rdV floor (coronal section) were counted. Seven 40-μm coronal serial sections (280μm) were counted between −1.515mm and −1.875mm from Bregma. On the rare occasion, a section would be lost in the collection process. The next section in the mouse sample was taken and counted (seven sections were counted total). For analysis of newborn Hu^+ neurons, for each section analyzed, Hu^+DAPI^+ and $Hu^+BrdU^+DAPI^+$ neurons within the MEm were counted in the region defined above, excluding cells of the uppermost focal plane to avoid oversampling. To determine the frequency of $BrdU^+$ cells expressing Hu, dual fluorescence-labeled sections were examined by confocal microscopy using a 20 x objective and 1.5 x digital zoom. For each marker and treatment condition, seven representative serial sections from each of four animals were examined. Sections were scored for double or triple labeling by manual examination of optical slices. Cells were considered positive for a given phenotypic marker when the marker-specific labeling was unambiguously associated with a $BrdU^+$ nucleus. Cells were spot-checked in all three dimensions by Z-stack using a 63x objective. Images of $Hu^+BrdU^+DAPI^+$ labeling in feeding conditions (Fig. 2, SFig. 4) were blinded prior to counting. Cells were corrected for number of optical slices and overcounting of large neurons with Abercrombie correction[16]. Cell counts are described in the text and figure legends as mean of several samples ± s.e.m., total cell counts, and the number of samples examined to derive those total cell counts.

Quantitative magnetic resonance spectroscopy and *in vivo* metabolic analysis

Female C57BL/6J mice maintained on a high-fat diet beginning at 5 weeks underwent irradiation (n=9) or sham procedure (n=9) at 5.5 weeks of age. At 10 weeks old, mice were placed in the EchoMRI-100 (Echo Medical Systems, Houston, Texas) scanner, which allows for the measurement of whole body fat mass, lean tissue mass, free water, and total body water in live animals with quantitative magnetic resonance spectroscopy.

A different cohort of female C57BL/6J mice maintained on a high-fat diet beginning at 4.5 weeks underwent irradiation (n=11) or sham procedure (n=12) at 5.5 weeks of age. Two weeks following treatment, mice were then tested in a Comprehensive Lab Animal Monitoring System (CLAMS, Columbus Instruments), for simultaneous measurements of powdered high-fat diet intake, physical activity (infrared beam breaks), and whole-body metabolic profile by indirect calorimetry. After several days of acclimation, mice were monitored for the following: rates of oxygen consumption (VO_2, ml/kg/hr) and carbon dioxide production (VCO_2) were measured for each chamber every 24 minutes throughout the study; respiratory exchange ratio (RER = VCO_2 / VO_2) was calculated by Oxymax software (v. 4.70) to estimate relative oxidation of carbohydrate (RER = 1.0) versus fat (RER approaching 0.7), not accounting for protein oxidation; rates of energy expenditure were calculated as EE = VO_2 x (3.815 + (1.232 x RER))[17], and normalized for subject body mass (kcals/kg/hr). Average metabolic values were calculated per subject and averaged across subjects for statistical analyses by paired, two-tailed test (unequal variance) for the

last day in the metabolic chamber (dark portion of day), when mice were most acclimated for metabolic testing.

Focal irradiation of ventrobasal hypothalamus

Radiation (10 Gy) was delivered using the Small Animal Radiation Research Platform (SARRP), a dedicated laboratory radiation device developed in-house[13]. The mouse was anesthetized using ketamine and placed on the robotically-controlled stage of the SARRP unit. A computed tomography (CT) was acquired with the SARRP (voxel size of 0.2 mm), and the 3rdV was identified on this scan. To confirm target visualization, a CT was acquired on mice using iodine contrast injected intrathecally which allows the ventricles to be directly visualized on CT images (n=3)[13]. From the dual iodine contrast CT analysis, an anatomical template was used for all following irradiation targeting of the median eminence. After the target was identified on CT, the mouse was moved under robotic control to align this target with the radiation delivery beam of the SARRP. Using a 1 mm diameter beam collimator, an arc technique was used to deliver 10 Gy to the target point[14]. Previous measurements indicate that this technique provides very low doses of radiation (<0.1 Gy) outside the 1 mm target. The area of the pituitary gland and surrounded structures is therefore effectively shielded from irradiation. The accuracy of the beam targeting has been measured in previous studies to be within 0.2 mm both in phantom tests [14] and in tissue sections[13]. As further confirmation for the present study, we performed immunohistochemical staining on three mice one-hour after irradiation against γH2Ax, the well-known histone protein that is an early marker of DNA double strand breaks[13]. This provides direct visualization of the radiation beam in tissue.

Sham controls were performed in parallel. Mice in this cohort were caged, transported to the procedure room, received the same anesthesia, and received similar amounts of ambient radiation coming from the SARRP as the irradiated cohort. Sham controls differed only in that they did not receive a direct radiation beam.

Statistical Analysis

Figures are shown as mean±standard error of the mean. Student’s t-test was employed, and corrected for multiple comparisons by using Dunn-Šidák correction.

Supplementary Material

Refer to Web version on PubMed Central for supplementary material.

Acknowledgments

We thank J. Nathans, S. Hattar, N. Gaiano, P. Achanta, C. Montojo, D. McClellan, T. Shimogori, T. Moran, E. Newman, M. Taylor, and W. Yap for comments on the manuscript. We also thank M. Bonaguidi, C. Montojo, J. Reyes, M. Armour, E. Velarde, N. Forbes-McBean, W.F. Han and the Johns Hopkins School of Medicine Microscope Facility for technical advice and assistance. This work was supported by NIH F31 NS063550 and an NSF Graduate Fellowship (to D.A.L.), a Basil O’Connor Starter Scholar Award and grants from the Klingenstein Fund and NARSAD (to S.B.). S.B. is a W.M. Keck Distinguished Young Scholar in Medical Research.

Literature Cited

1. Kokoeva MV, Yin H, Flier JS. Science. 2005; 310:679–683. [PubMed: 16254185]
2. Pierce AA, Xu AW. J Neurosci. 2010; 30:723–730. [PubMed: 20071537]
3. Xu Y, et al. Exp Neurol. 2005; 192:251–264. [PubMed: 15755543]
4. Mathew TC. Anat Histol Embryol. 2008; 37:9–18. [PubMed: 18197894]
5. Rodriguez EM, et al. Int Rev Cytol. 2005; 247:89–164. [PubMed: 16344112]
6. Shimogori T, et al. Nat Neurosci. 2010; 13:767–775. [PubMed: 20436479]
7. Miller I, Ronnett GV, Moran TH, Aja S. Neuroreport. 2004; 15:925–929. [PubMed: 15073544]
8. Cowley MA, et al. Nature. 2001; 411:480–484. [PubMed: 11373681]
9. Simerly RB. Physiol Behav. 2008; 94:79–89. [PubMed: 18262209]
10. Balordi F, Fishell G. J Neurosci. 2007; 27:14248–14259. [PubMed: 18160632]
11. Srinivas S, et al. BMC Dev Biol. 2001; 1:4. [PubMed: 11299042]
12. Masahira N, et al. Dev Biol. 2006; 293:358–369. [PubMed: 16581057]
13. Ford EC, et al. Radiat Res. 2011; 175:774–783. [PubMed: 21449714]
14. Matinfar M, et al. Med Image Comput Comput Assist Interv. 2007; 10:926–934. [PubMed: 18044657]
15. d'Avella D, et al. J Neurosurg. 1994; 81:774–779. [PubMed: 7931625]
16. Abercrombie M. Anat Rec. 1946; 94:239–247. [PubMed: 21015608]
17. Lusk, G. The elements of the science of nutrition. 4. WB Saunders; Philadelphia, PA: 1928.

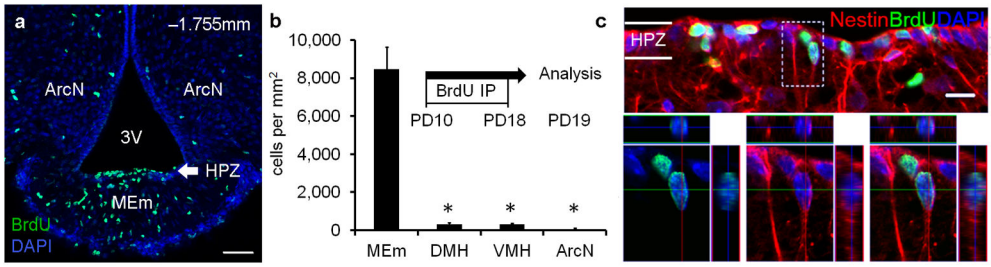

Figure 1. Hypothalamic Proliferative Zone

PD19 mice received BrdU (PD10 18), and coronal ventrobasal hypothalamic sections were examined for BrdU immunostaining. **(a)** Hypothalamic proliferative zone (HPZ): enriched $BrdU^+$ cell population along the MEm ependymal layer of third ventricle (3V) floor. **(b)** Quantification of $BrdU^+$ ependymal layer cells juxtaposing hypothalamic nuclei (n=4; mean ±s.e.m.; *=p<0.01): median eminence (MEm: 8488.5±1134.8 cells/mm^2), arcuate nucleus (ArcN: 66.5±54.0 cells/mm^2), ventromedial nucleus (VMH: 298.1±58.3 cells/mm^2), dorsomedial nucleus (DMH: 307.6±90.3 cells/mm^2). **(c)** HPZ $BrdU^+$ cells are β2-tanycytes: ependymal layer position, radial-glial like morphology, and co-expression of tanycyte-enriched markers like Nestin. Dashed box: higher magnification z-stack reconstruction. Sections counterstained with DAPI (blue), a nuclear marker. Scale bar = 50μm (a); 10μm (c).

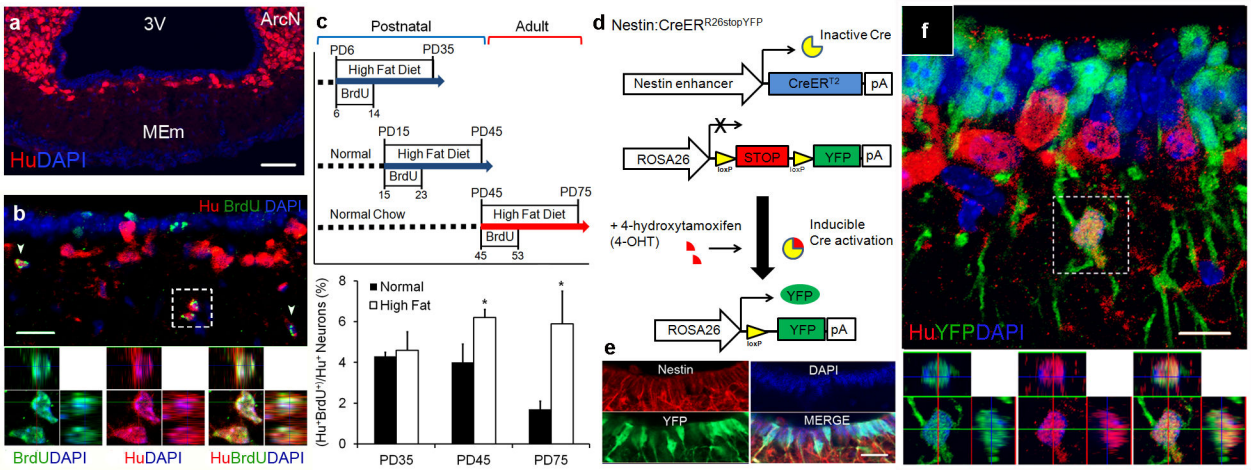

Figure 2. The median eminence is a neurogenic niche

(a) MEm neuronal distribution in PD35 mice. **(b)** PD35 mice received BrdU (PD10 18); MEm immunostained for BrdU and pan-neuronal marker Hu. Hu^+BrdU^+ co-expression adjacent to HPZ. **(c)** Age and diet-dependent effects of MEm neurogenesis. Newborn Hu^+BrdU^+ MEm neurons quantified 1 month following BrdU administration. (n=4; mean ±s.e.m.; *=p<0.05) **(d)** Nestin:$CreER^{R26stopYFP}$ mice permanently labels tanycytes and their progeny with yellow fluorescent protein (YFP) after 4-hydroxytamoxifen (4-OHT) induction. **(e)** PD7 Nestin:$CreER^{R26stopYFP}$ mice treated with 4-OHT 72 hrs prior demonstrate specificity of tanycytic labeling via co-expression of YFP and $Nestin^+$ tanycytes. **(f)** PD35 Nestin:$CreER^{R26stopYFP}$ mice were 4-OHT induced at PD4. Hu^+YFP^+ neurons present following 1 month post-induction, but not following a 72 hr interval (SFig. 5g). Sections counterstained with DAPI (blue), a nuclear marker. Scale bars: 50μm (a); 20μm (b,e); 10μm (f).

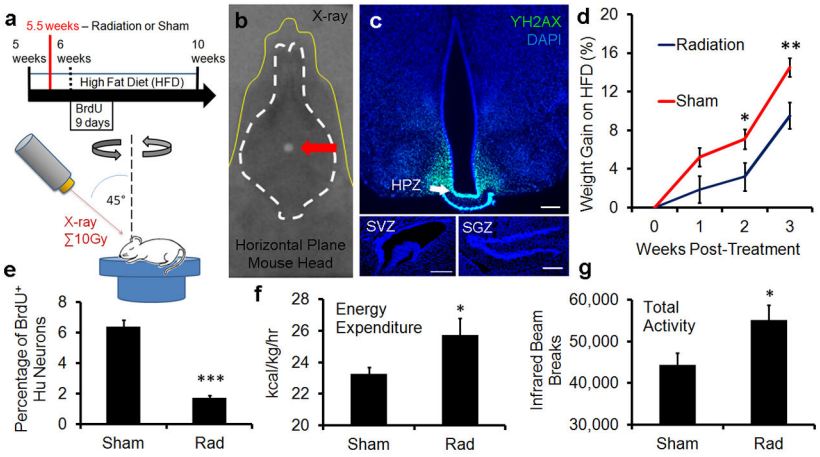

Figure 3. Median eminence neurogenesis regulates metabolism

(a) Experimental diagram of CT-guided irradiation of HPZ. **(b)** Superimposition of dosimetry-film acquired with 1mm radiation beam in phantom with an X-ray of a real mouse subject (yellow line). White circle (arrow) indicates 10Gy radiation dose focally targeted towards HPZ. **(c)** Radiation targeting accuracy confirmed by γH2AX immunostaining, an indicator of radiation dose. γH2AX immunostaining limited to the HPZ within the ventrobasal hypothalamus. No radiation exposure observed within the SVZ and the SGZ. Scale bar = 200μm **(d)** Attenuated weight gain in HFD-fed irradiated mice compared with parallel sham controls (n=9). **(e)** Irradiation inhibits MEm neurogenesis by ~85% (n=4). **(f)** Higher energy expenditure observed in irradiated mice (n=11). **(g)** Higher total activity observed in irradiated mice (n=11). mean±s.e.m *=p<0.05; **=p<0.01